Stoichiometry of lipid interactions with transmembrane proteins—Deduced from the 3D structures

TIBOR PÁLI,[1,2] DENYS BASHTOVYY,[2] AND DEREK MARSH[1]

[1]Max-Planck-Institut für biophysikalische Chemie, Abt. Spektroskopie, 37070 Göttingen, Germany
[2]Institute of Biophysics, Biological Research Centre, H-6701 Szeged, Hungary

(RECEIVED December 9, 2005; FINAL REVISION February 2, 2006; ACCEPTED February 16, 2006)

Abstract

The stoichiometry of the first shell of lipids interacting with a transmembrane protein is defined operationally by the population of spin-labeled lipid chains whose motion is restricted directly by the protein. Interaction stoichiometries have been determined experimentally for a wide range of α-helical integral membrane proteins by using spin-label ESR spectroscopy. Here, we determine the spatially defined number of first-shell lipids at the hydrophobic perimeter of integral membrane proteins whose 3D structure has been determined by X-ray crystallography and lipid–protein interactions characterized by spin-labeling. Molecular modeling is used to build a single shell of lipids surrounding transmembrane structures derived from the PDB. Constrained energy optimization of the protein–lipid assemblies is performed by molecular mechanics. For relatively small proteins (up to 7–12 transmembrane helices), the geometrical first shell corresponds to that defined experimentally by perturbation of the lipid-chain dynamics. For larger, multi-subunit α-helical proteins, the lipids perturbed directly by the protein may either exceed or be less in number than those that can be accommodated at the intramembranous perimeter. In these latter cases, the motionally restricted spin-labeled lipids can be augmented by intercalation, or can correspond to a specific subpopulation at the protein interface, respectively. For monomeric β-barrel proteins, the geometrical lipid stoichiometry corresponds to that determined from lipid mobility for a 22-stranded barrel, but fewer lipids are motionally restricted than can be accommodated around an eight-stranded barrel. Deviations from the geometrical first shell, in the β-barrel case, are for the smaller protein with a highly curved barrel.

Keywords: integral proteins; lipid–protein interactions; boundary lipid; transmembrane α-helices; transmembrane β-barrels

Extensive series of spin-label electron spin resonance (ESR) studies with reconstituted integral membrane proteins have revealed that a constant number of lipids are motionally restricted by direct interaction with each protein, irrespective of the total lipid content of the membrane (for review, see Marsh and Horváth 1998). For example, such lipid/protein titrations have been performed with cytochrome *c* oxidase (Knowles et al. 1979), Na^+,K^+-ATPase (Brotherus et al. 1981), nicotinic acetylcholine receptor (Ellena et al. 1983), Ca^{2+}-ATPase (Silvius et al. 1984), myelin proteolipid protein (Brophy et al. 1984), rhodopsin (Ryba et al. 1987), ADP/ATP carrier (Horváth et al. 1990), M13 phage coat protein (Peelen et al. 1992), and phospholamban (Cornea et al. 1997; Arora et al. 2003). In an operational sense, therefore, the fixed stoichiometry of lipids interacting directly with the protein may be defined as a first shell at the intramembranous perimeter of the protein. This first shell of motionally restricted lipids

Reprint requests to: Derek Marsh, Max-Planck-Institut für biophysikalische Chemie, Abt. Spektroskopie, 37070 Göttingen, Germany; e-mail: dmarsh@gwdg.de; fax: 49-551-201-1501.

Article and publication are at http://www.proteinscience.org/cgi/doi/10.1110/ps.052021406.

exchanges with the surrounding bilayer lipids at an off-rate in the range 1–10 MHz, depending on the protein and on the thermodynamic affinity of the lipid species (Marsh and Horváth 1998). On the time scale of a typical ^{2}H-NMR experiment, lipids in the first shell are in rapid exchange with the fluid bilayer pool and therefore are not resolved in the NMR spectra from deuterated lipids (e.g., Oldfield 1982; Bloom and Smith 1985). It is the faster characteristic time scale of nitroxide ESR, relative to NMR, that allows lipid stoichiometries (and specificities) to be determined by spin-label methods.

The stoichiometry of lipid–protein interaction is important not only for structural reasons, but also because the first shell of lipids is responsible for sealing the protein into the membrane and hence maintaining the permeability barriers in the cell. The first-shell lipids are also those that solvate the protein in the membrane and provide the interface with the fluid lipid environment that is essential to the function of many membrane enzymes (see, e.g., Hesketh et al. 1976; Fajer et al. 1989). In several cases, the first shell or annulus of lipids also represents the minimum number of lipids required to support activity of the transmembrane protein (see, e.g., Hesketh et al. 1976; Knowles et al. 1979; Jones et al. 1988).

If the operational definition of the first shell of lipids corresponds also to the spatial definition, it is expected that this fixed lipid stoichiometry will be related directly to the transmembrane structure, and degree of oligomerization, of the protein. From simple geometric considerations for helical sandwiches or regular polygons of α-helices, it is predicted that the number of perimeter lipids, N_b (on both sides of the bilayer), increases linearly with the number, n_α, of transmembrane helices per monomer (Marsh 1997):

$$N_b = \pi(D_\alpha/d_{ch} + 1) + n_\alpha D_\alpha/d_{ch} \qquad (1)$$

where D_α and d_{ch} are the diameters of an α-helix and a lipid chain, respectively, and $n_\alpha > 1$. For a single transmembrane helix: $N_b = \pi(D_\alpha/d_{ch} + 1)$. Equation 1 predicts reasonably well the stoichiometry of lipid interaction with relatively small monomeric α-helical bundles, notably the archetypal seven-helix sandwich of rhodopsin (Marsh 1997). To a lesser extent, an extended version of Equation 1 that preserves the helical packing motif for protein oligomers has proved useful for describing the lipid stoichiometry of oligomers composed of small monomers. The stoichiometry per monomer is then given from Equation 1 by:

$$N_b^{(1)} = \left(\pi/n_{agg}\right)(D_\alpha/d_{ch} + 1) + n_\alpha D_\alpha/d_{ch} \qquad (2)$$

where n_{agg} is the number of monomers per oligomer. Reasonable performance by Equation 2 is achieved in the case of hexamers of four-helix proteolipids (Brophy et al. 1984; Páli et al. 1995) and the oligomers of phospholamban (Arora et al. 2003). On the other hand, the simple helical packing described by Equations 1 and 2 is not appropriate in the case of large multi-subunit proteins, such as the nicotinic acetylcholine receptor and cytochrome *c* oxidase (Marsh 1997).

In recent years, the structures of an increasing number of transmembrane proteins have been determined by X-ray diffraction methods. We are therefore now in a position to compare the number of first-shell lipids that are defined by their dynamic properties using ESR with predictions from the intramembranous geometry of the protein. The purpose of the present paper is to determine the number of lipids that can be accommodated around the transmembrane section of the protein by using molecular mechanics and model building. The modeling approach is necessary because, in general, only a few lipids (or more frequently no lipids) are resolved in the crystal structures.

Previously, the molecular mechanics procedure was applied successfully to lipidation of the M13 phage coat protein, when analyzing results from site-directed spin-labeling of the protein (Bashtovyy et al. 2001). Twelve dioleoyl phosphatidylcholine molecules can be accommodated around the single transmembrane helix of this bitopic protein. This latter value agrees well with the number of motionally restricted lipids associated with the L37A mutant of phospholamban, for which mutation of the leucine zipper in the single transmembrane helix prevents oligomer formation (Cornea et al. 1997). The wild-type M13 coat protein itself forms oligomers in dioleoyl phosphatidylcholine bilayers (Peelen et al. 1992).

Recently, the first determination of the stoichiometries for motionally restricted lipids interacting with β-barrel transmembrane proteins has been made with spin-label ESR spectroscopy (Ramakrishnan et al. 2004). Structures of this type of transmembrane protein already have been characterized extensively by X-ray diffraction (Schulz 2002). Therefore, we have also determined the geometric first-shell lipid stoichiometries for this class of outer membrane protein, by using the molecular-mechanics modeling approach.

Results and Discussion

Figure 1 shows the structure of bovine rhodopsin (PDB code 1L9H) (Okada et al. 2002), together with space-filling models of dimyristoyl phosphatidylcholine (myr_2PtdCho). The lipid chains are shortened from their all-*trans* length (by using a tether function in the program Sculpt; Surles et al. 1994) and positioned vertically around the protein to achieve good hydrophobic matching. (Chain shortening was necessary to prevent overlap of lipids from the two halves of the bilayer.) The chains are close-packed around the protein by applying external inward-directed forces to each lipid atom that are referred to as ''springs'' in the Sculpt program. The structure is energy-minimized within

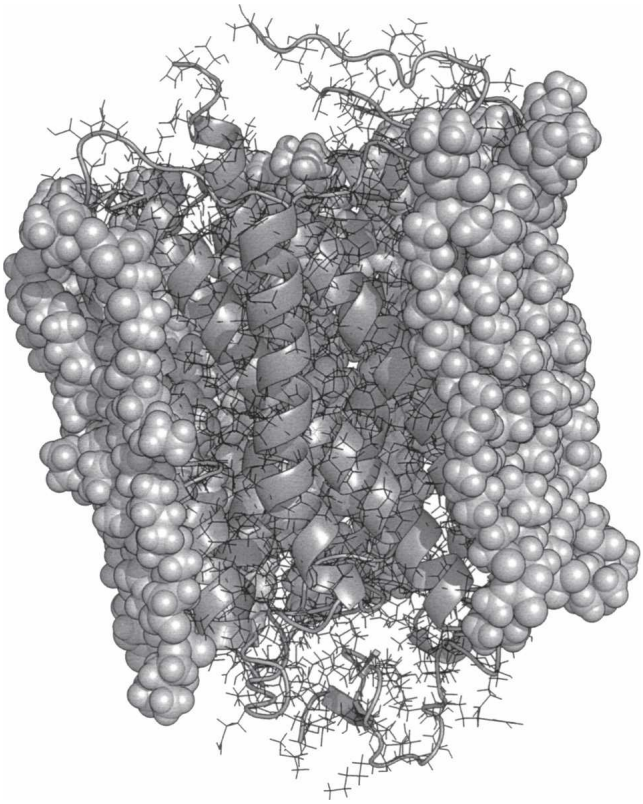

Figure 1. Crystal structure of bovine rhodopsin (PDB code 1L9H) (Okada et al. 2002) in ribbon and wire-frame representation, surrounded by a single bilayer shell of energy-minimized myr_2PtdCho lipids (see text). For clarity, only part of the lipid shell is shown, in space-filling representation.

Sculpt by using the default force field, with the protein backbone kept fixed. The size of the inward forces applied to the lipids is chosen to give the deepest energy minimum (excluding the energy of the springs; see Materials and Methods).

The number of dimyristoyl phosphatidylcholine lipids that can be accommodated around the intramembranous perimeter of the rhodopsin structure in Figure 1 is $\sim 27 \pm 2$. For comparison, the number of lipids motionally restricted by bovine rhodopsin reconstituted in dimyristoyl phosphatidylcholine bilayers is 22 ± 2 (Ryba et al. 1987). The corresponding values in native membranes are 25 ± 3 and 23 ± 2 lipids per rhodopsin for bovine and frog rod outer segment discs, respectively (Watts et al. 1979; Pates et al. 1985). The prediction from Equation 1 is $N_b = 24$ for a seven-helix sandwich. Thus, all estimates agree reasonably well, in this case. The motionally restricted lipid population that is detected by spin-label ESR is approximately sufficient to constitute a complete shell of lipids surrounding the intramembranous perimeter of rhodopsin. Also, Equation 1 gives a reasonable approximation for helical sandwiches such as rhodopsin (i.e., for $n_\alpha \sim 7$), even when the helices are tilted somewhat.

As a further illustration for a relatively small α-helical protein, the structure of the mitochondrial ADP/ATP exchange carrier surrounded by a first shell of myr_2PtdCho lipids is shown in Figure 2. This is a protein with six transmembrane helices that is monomeric in its crystalline form (PDB code 1OKC) (Pebay-Peyroula et al. 2003). Twenty-eight lipids can be accommodated around the intramembranous perimeter of this protein, as deduced from the molecular mechanics procedure. For comparison, the stoichiometry of motionally restricted lipids deduced by spin-label ESR for the ADP/ATP carrier reconstituted in egg phosphatidylcholine is $N_b = 28 \pm 2$ per protein monomer (Horváth et al. 1990). Again, the stoichiometry of motionally restricted lipids corresponds to the physical intramembrane perimeter of the protein.

Table 1 gives the numbers of first-shell lipids that are obtained for the various α-helical transmembrane proteins that have been subjected to ESR analysis and have structures in the Protein Data Bank (PDB), by using the methods described above. Generally, for the proteins in Table 1, any asymmetry between the two bilayer leaflets is not much greater than the uncertainty in the total number of lipids that could be accommodated around the protein. An asymmetry of one to two lipids is estimated for cytochrome oxidase and cytochrome reductase, and

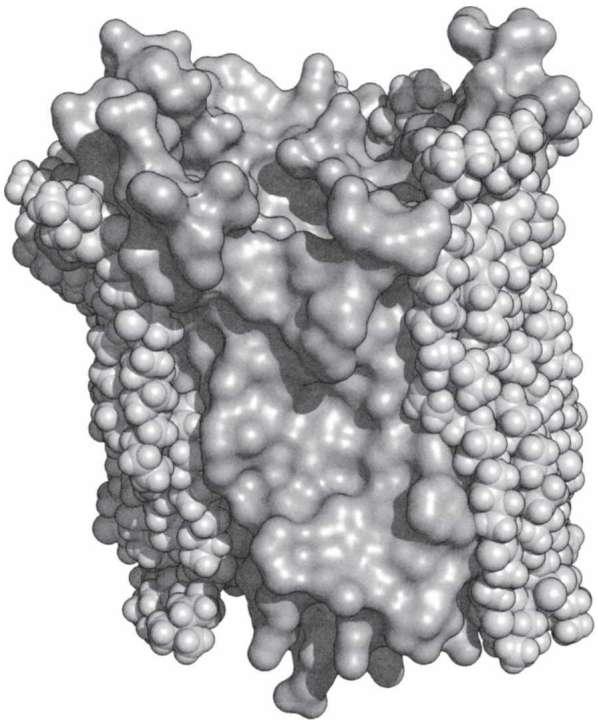

Figure 2. Van der Waals surface from the crystal structure of the mitochondrial ADP-ATP carrier (PDB code 1OKC) (Pebay-Peyroula et al. 2003), surrounded by a single bilayer shell of energy-minimized myr_2PtdCho lipids. For clarity, only part of the lipid shell is shown, in space-filling representation.

Table 1. *The number of dimyristoyl phosphatidylcholine molecules, N_b, that can be accommodated in a bilayer around the intramembranous perimeter of the 3D structures of integral proteins*

Protein[a]	PDB code	Ref.	N_b (mol/mol)[b]
Bovine rhodopsin [Rho]	1L9H	Okada et al. 2002	27 ± 2 (22–25)
ADP-ATP carrier [ADP]	1OKC	Pebay-Peyroula et al. 2003	28 ± 2 (25)
Bacteriorhodopsin (*Halobacterium salinarum*) [bR]	1C3W	Luecke et al. 1999	25 ± 2
KcsA K^+-channel [KcsA]	1K4C	Valiyaveetil et al. 2002	33 ± 3
Ca^{2+}-ATPase [Ca]	1EUL	Toyoshima et al. 2000	28 ± 4 (22–24)
Bovine cytochrome *c* reductase (bc_1 complex) [CR]	1L0L	Gao et al. 2002	46 ± 4 (38)
Nicotinic acetylcholine receptor [AChR]	1OED	Miyazawa et al. 2003	52 ± 4 (40)
Bovine cytochrome *c* oxidase [CO][c]	1V54	Tsukihara et al. 2003	86 ± 8 (56) (dimer)[d] 57 ± 4 (monomer)[e]
OmpA (*Escherichia coli*)	1QJP	Pautsch and Schulz 2000	20 ± 2 (11)
FhuA (*E. coli*)	2FCP	Ferguson et al. 1998	34 ± 2 (32)

[a] The abbreviations used in Figure 3 are enclosed in square brackets.
[b] The numbers of motionally restricted lipids per protein monomer, determined from spin-label ESR spectroscopy, are given in parentheses after the corresponding entry for N_b (for references, see Marsh and Horváth 1998; Ramakrishnan et al. 2004).
[c] Corrected for uncovered surface in model, but some overlap with lipids in invaginations (see text).
[d] Lipids at the outer perimeter. Approximately four to six more lipids can be accommodated at the protein surface within the central cavity of the dimer.
[e] Monomer derived from dimer structure.

of approximately one lipid for Ca^{2+}-ATPase and the KcsA channel. Figure 3 compares the stoichiometries of motionally restricted lipids associated with α-helical integral proteins that are determined by spin-label ESR with those predicted by the molecular modeling. The geometric predictions of Equations 1 and 2 for monomers and hexamers also are shown, by the solid and dotted lines, respectively. The number of first-shell lipids that can be accommodated around bacteriorhodopsin (N_b = 24–25) is slightly smaller than for rhodopsin because the helices of the seven-helix bundle are tilted less in bacteriorhodopsin than in the G-protein-coupled visual receptor. Both are in approximate accord with spin-label ESR experiments and estimates from Equation 1.

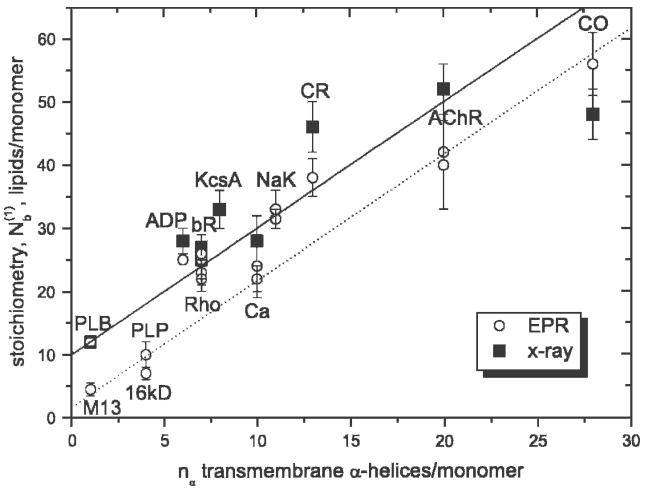

Figure 3. Number, N_b, of first-shell lipids interacting with different integral proteins composed of n_α transmembrane helices per monomer. Solid squares correspond to the first shell of lipids surrounding the X-ray structure of the protein, as determined by model building. Open circles correspond to the motionally restricted lipids that are resolved by ESR spectroscopy; multiple entries correspond to different experimental reports (see Marsh and Horváth 1998 for references). (Solid line) Prediction of Equation 1 for helical sandwiches; (dotted line) prediction of Equation 2 for hexamers (n_{agg} = 6); (M13) M13 phage coat protein; (PLB) L37A mutant of phospholamban; (PLP) myelin proteolipid protein; (16 kD) 16-kDa proteolipid from *Nephrops norvegicus*; (ADP) ADP-ATP carrier; (Rho) rhodopsin; (Ca) Ca^{2+}-ATPase; (NaK) Na^+,K^+-ATPase; (CR) cytochrome *c* reductase; (AChR) nicotinic acetylcholine receptor; (CO) cytochrome *c* oxidase.

For the SERCA Ca^{2+}-ATPase, which consists of a single, large subunit that contains 10 transmembrane helices, the number of lipids motionally restricted is less than the number of first-shell lipids that is obtained by molecular modeling. In this case, the number of first-shell lipids lies between the stoichiometries of the Ca^{2+}-ATPase and the Na^+,K^+-ATPase, both of which are P-type ATPases and are thought to have the same number of transmembrane helices, except for the extra single transmembrane domain contributed by the β-subunit of the Na^+,K^+-ATPase. The reduction in number of motionally restricted lipids for the Ca^{2+}-ATPase may possibly be attributable to dimerization. For the multi-subunit proteins—cytochrome *c* reductase, nicotinic acetylcholine receptor, and cytochrome *c* oxidase—the stoichiometry of motionally restricted lipids found by spin-label ESR also differs considerably from the intramembranous perimeter of the protein that is determined from molecular mechanics and modeling.

Bovine cytochrome *c* reductase consists of 11 subunits, six of which contribute a total of 13 transmembrane helices per monomer. The asymmetric unit of bovine cytochrome *c* reductase in PDB file 1L0L is a monomer,

although the active membrane species is thought to be a dimer (Gao et al. 2002). In PDB file 1PP9 for bovine cytochrome *c* reductase at marginally higher resolution (Huang et al. 2005), the asymmetric unit is a dimer, but the entire intramembranous perimeter of each monomer appears still to be accessible to lipid. The intramembranous perimeter of the structure in PDB file 1L0L can accommodate more lipids than are found to be motionally restricted, per monomer, by ESR spectroscopy. Possibly interactions within the functionally active dimer nonetheless limit the stoichiometry of motionally restricted lipids.

The nicotinic acetylcholine receptor is a heteropentamer composed of four homologous subunits, $\alpha_2\beta\gamma\delta$, each constituting a transmembrane four-helix bundle (PDB code 1OED) (Miyazawa et al. 2003). The stoichiometry of motionally restricted lipids for the receptor reconstituted in dioleoyl phosphatidylcholine is $\sim 40 \pm 7$ lipids per protomer (Ellena et al. 1983). A similar value has also been estimated for the stoichiometry in native receptor-rich membranes from *Torpedo* electroplax (Mantripragada et al. 2003). This value is less than that found for the intramembranous perimeter of the $\alpha_2\beta\gamma\delta$ protomer (see Table 1). As is seen from Figure 4, the transmembrane section of the protein has an extremely angular, star-shaped cross-section. Lipid packing at the intramembranous surface of the protein is considerably less regular than that at the smoother surfaces of the smaller proteins that have a helical-sandwich structure (cf. Figs. 1 and 2). Possibly the intramembranous surfaces at the apices of the star, which correspond to a single transmembrane helix from each subunit, are insufficient to restrict lipid-chain motion appreciably. In several instances, single transmembrane helices are not capable of motionally restricting lipids in the direct way found invariably for polytopic α-helical proteins (Pérez-Gil et al. 1995; de Planque et al. 1998, 1999). Phospholamban is possibly an exception (Cornea et al. 1997; Arora et al. 2003). Therefore, the motionally restricted lipids detected by spin-label ESR spectroscopy for the nicotinic acetylcholine receptor may constitute only those perimeter lipids that are located at the extended surfaces, along the arms of the star (cf. Fig. 4). An alternative explanation for the low stoichiometry of motionally restricted lipids with the acetylcholine receptor could be oligomerization, via S–S cross-linking (Zingsheim et al. 1982) at the helices forming the apices of the transmembrane cross-section. This would also result in only the extended surfaces along the arms of the star giving rise to motional restriction of the lipids.

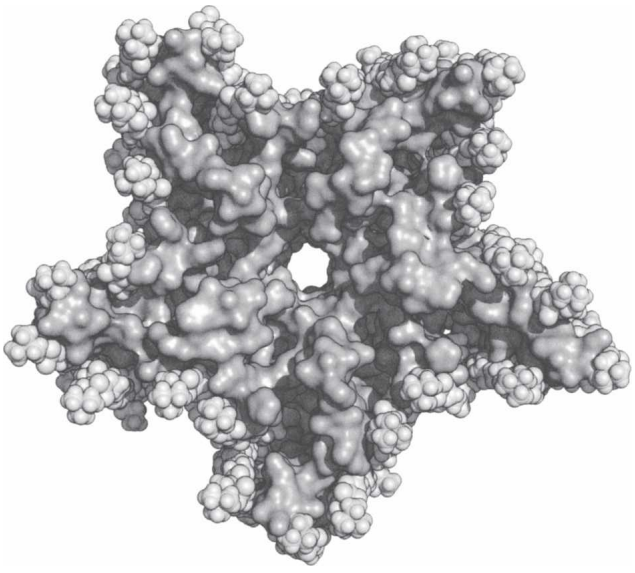

Figure 4. Van der Waals surface for the transmembrane domain in the 3D structure of the nicotinic acetylcholine receptor (PDB code 1OED) (Miyazawa et al. 2003). The structure is viewed along the membrane normal. An energy-minimized first shell of lipids at the intramembranous perimeter of the protein is shown, in space-filling representation.

Bovine cytochrome *c* oxidase is composed of 13 subunits of differing sizes that contribute a total of 28 transmembrane helices per monomer (PDB code 1V54) (Tsukihara et al. 2003). It is the largest integral protein for which the lipid stoichiometry has been determined by spin-label ESR spectroscopy. The structure of the transmembrane domain of bovine cytochrome *c* oxidase is shown in Figure 5. For ease of handling, chains e, f, h, r, s, and u of the extramembranous sector that does not contact lipid are omitted here from the PDB structure. The protein is dimeric in the crystal, and some lipids are occluded within the central cavity at the dimer interface (cf. Fig. 5). In addition, it is seen that the hydrophobic surface of the protein is considerably invaginated, in contrast to the rather smooth intramembranous surface of the helical sandwiches in Figures 1 and 2. This introduces some imprecision in definition of the geometric first shell, because a continuous lipid shell would cover some lipids occluded within invaginations. The procedure for optimizing the energy of the lipid contacts results in some such lipid overlaps before all protrusions of the protein surface are covered completely with lipids. In the structure shown in Figure 5, 37 energy-optimized myr_2PtdCho lipids per monomer are located around the outer perimeter of the dimer. There are several partial overlaps with lipids in invaginations. Nevertheless, not all of the outer intramembranous surface of the protein is covered with lipids. It is estimated that an additional six diacyl lipids per monomer would be required to cover the protein surface entirely. Making this correction produces the value given for the outer perimeter of the cytochrome oxidase dimer in Table 1, namely, $N_b \approx 86 \pm 8$ lipids per dimer. However, the chain overlaps in Figure 5 constitute approximately four to five diacyl lipids that are effectively in the second shell.

Unfortunately, the strategy used for energy optimizing the lipids at the outer perimeter cannot be applied to

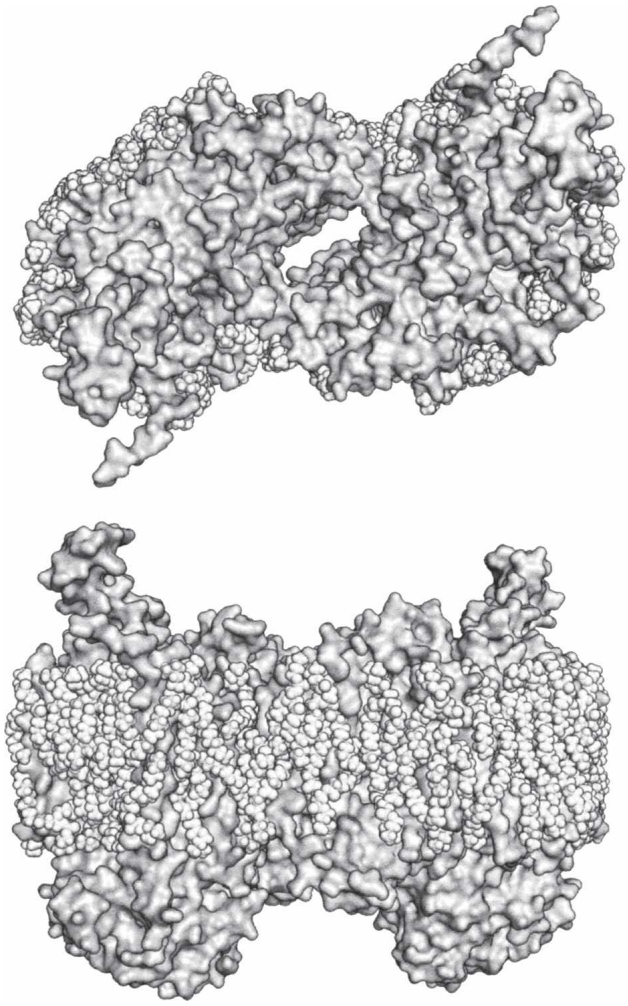

Figure 5. Van der Waals surface from the crystal structure of the intramembrane domain of the bovine cytochrome *c* oxidase dimer (PDB code 1V54) (Tsukihara et al. 2003), with energy-minimized myr_2PtdCho lipids at the outer intramembranous surface (space-filling representation). Protein chains e, f, h, r, s, and u, and all endogenous lipids and detergent have been removed from the PDB structure. The *upper* panel shows a top view, approximately along the membrane normal, and the *lower* panel shows a side view from within the plane of the membrane.

the internal cavity of the cytochrome oxidase dimer. By examining the positions of the endogenous lipids (particularly phosphatidylethanolamine and phosphatidylglycerol) in the crystal structure, it is estimated that an additional four to six lipids per monomer could be situated at the protein surface in this central region. Therefore, the net geometric stoichiometry for the dimer is approximately $N_b^{(1)} = N_b/2 \approx 47$–$49$ lipids per monomer. The latter estimate corresponds to the value that is given for cytochrome oxidase in Figure 3. However, this value is reduced to 42–45 lipids per monomer if the chain overlaps in Figure 5 are excluded. For a putative monomer derived from the dimer crystal structure, $\sim 57 \pm 4$ lipids can be accommodated around the entire surface, where the difference represents lipids that are excluded at the dimer interface.

For comparison with the geometric lipid stoichiometry evaluated by modeling, the number of motionally restricted spin-labeled lipids found for bovine cytochrome *c* oxidase reconstituted in dimyristoyl phosphatidylglycerol is $N_b = 55 \pm 4$ per monomer (Kleinschmidt et al. 1998). A similar value of $N_b = 56 \pm 5$ lipids per monomer is also found for the homologous yeast cytochrome *c* oxidase reconstituted in myr_2PtdCho (Knowles et al. 1979). Note that in the reconstituted systems, the cardiolipin and other endogenous lipid that is found in the crystals of bovine cytochrome *c* oxidase is completely replaced with the reconstituting lipid by repeated exchanges against a large excess of the substituting lipid, mediated by cholate (Watts et al. 1978; Powell et al. 1985). The number of motionally restricted lipids therefore exceeds the above geometric first-shell stoichiometry of the cytochrome oxidase dimer if lipid overlaps are eliminated. Presumably, the difference represents those extra lipids that are covering lipids already filling invaginations, and these lipids are also motionally restricted.

Figure 6 shows the β-barrel structure of the Fe-siderophore transporter FhuA from the outer membrane of *Escherichia coli* (PDB code 2FCP) (Ferguson et al. 1998), surrounded by a bilayer shell of dimyristoyl

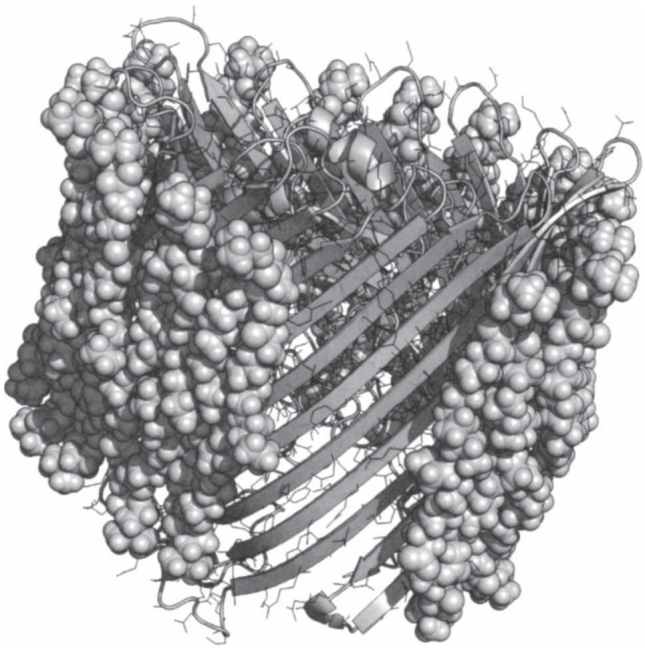

Figure 6. Crystal structure of *E. coli* outer membrane protein FhuA (PDB code 2FCP) (Ferguson et al. 1998), in ribbon and wire-frame representation, surrounded by a single bilayer shell of energy-minimized myr_2PtdCho lipids. For clarity, only part of the lipid shell is shown, in space-filling representation.

phosphatidylcholine lipids. The FhuA barrel is composed of 22 antiparallel next-neighbor β-strands, and the protein is monomeric. The lipids are positioned vertically relative to the two belts of aromatic residues that are situated at the opposing polar–apolar interfaces of the membrane. Using the molecular mechanics procedures already described for α-helical proteins, 34 ± 2 lipids can be fitted around the intramembranous perimeter of the FhuA structure that is given in Figure 6. For comparison, the number of lipids that are motionally restricted by FhuA reconstituted in dimyristoyl phosphatidylglycerol is $N_b = 32$ per protein monomer (Ramakrishnan et al. 2004). This is close to the number of lipids that can be accommodated around the intramembranous perimeter of FhuA and agrees also with the perimeter length of 31 lipids that is estimated from the overall dimensions of the protein. In fact, the stoichiometry for a large β-barrel such as FhuA approximates to that for an extended, planar β-sheet. For the latter, the number of diacyl bilayer lipids that can be accommodated at one intramembranous surface is determined by the number of β-strands, n_β, and the geometrical parameters of the β-sheet (Marsh 1997):

$$N_b = n_\beta D_\beta / (d_{ch} \cos \theta_\beta) \quad (3)$$

where θ_β is the strand tilt within the sheet, $D_\beta = 0.47$ nm (Fraser and MacRae 1973) is the interstrand separation, and $d_{ch} = 0.48$ nm (Marsh 1990) is the width of a lipid chain. For FhuA ($n_\beta = 22$), the strand tilt is $\theta_\beta = 38.3°$ (Páli and Marsh 2001), which gives a stoichiometry of $N_b = 27$ lipids, which is not much smaller than the perimeter length of the β-barrel.

Applying a procedure such as that illustrated in Figure 6 to the much smaller eight-stranded β-barrel of the outer membrane protein OmpA from *E. coli* yields a geometrical first shell of 20 ± 2 lipids per protein monomer. A considerably smaller value of $N_b = 11$ is obtained by ESR spectroscopy for the number of spin-labeled lipids that are motionally restricted by the OmpA monomer (Ramakrishnan et al. 2004). Estimating the perimeter length from the overall dimensions of the OmpA barrel yields a value of 19 lipids per monomer, similar to that established directly here by molecular modeling. Thus, the number of lipids that directly are restricted in their motion corresponds to the geometrical perimeter for a large β-barrel, FhuA, but is significantly smaller than the geometrical stoichiometry for a small β-barrel, OmpA. Presumably this is a result of the highly curved surface of the smaller barrel, which therefore cannot interact optimally with all lipids that are in direct contact.

Conclusion

In conclusion, it should be emphasized that the strategy adopted in the molecular modeling is directed solely at determining the lipid stoichiometry. The aim is to ensure complete filling of volume at the lipid–protein interface, for good hydrophobic matching, irrespective of chain configuration. In reality, there may be a mixing of chains between first and second shells, but this does not alter the net stoichiometry of chain segments directly contacting the protein.

For relatively small α-helical proteins (with up to seven to 12 transmembrane helices), the number of motionally restricted lipids corresponds rather well with the geometric first shell. These proteins approximate in their transmembrane structure to α-helical sandwiches. For larger, multi-subunit α-helical proteins, the intramembranous surface is less regular than in the α-helical sandwiches, and the number of motionally restricted lipids either may exceed (cytochrome oxidase), or be less than (acetylcholine receptor), the geometrical perimeter shell defined by lipid close packing. From the limited data available, it seems that the situation is the reverse for β-barrel integral proteins. Large β-barrels approximate to extended planar β-sheets and fully restrict the contacting lipids, whereas small β-barrels are not able completely to restrict all lipids that are in immediate contact with the highly curved intramembranous surface of the protein.

Materials and methods

Protein structures

Coordinates of all protein structures were obtained from the Research Collaboratory for Structural Bioinformatics protein database (PDB) (Berman et al. 2000). Generally, where alternative structures are available, that determined at highest resolution was used.

Spin-label ESR data

The stoichiometry, N_b, of motionally restricted lipids interacting with the transmembrane domain of integral proteins was determined by ESR difference spectroscopy (Marsh 1982) with lipids spin-labeled on the 14-C atom of the *sn*-2 chain at probe concentrations. All membranes were either in the fluid phase or in the liquid-ordered phase. For proteins in reconstituted membranes, the values of N_b were determined by lipid–protein titration according to the following relation for equilibrium exchange association (Marsh 1985):

$$N_b = \frac{n_t f}{K_r + (1 - K_r) f} \quad (4)$$

where f is the fraction of motionally restricted spin-labeled lipids, n_t is the total lipid/protein ratio, and K_r is the association constant of the spin-labeled lipid relative to the host lipid used for reconstitution. Both N_b and K_r are determined by varying n_t, in the range $n_t > N_b$. It is found that $K_r \approx 1$ for spin-labeled phosphatidylcholine relative to unlabeled phosphatidylcholine (Knowles et al. 1979; Ellena et al. 1983; Brophy et al. 1984;

Ryba et al. 1987; Horváth et al. 1990), and for spin-labeled phosphatidylglycerol relative to unlabeled phosphatidylglycerol (Sankaram et al. 1991; Kleinschmidt et al. 1998). For proteins in natural membranes, the stoichiometries were determined with spin-labeled phosphatidylcholine, assuming that $K_r = 1$, because phosphatidylcholine is the majority lipid in the native membranes. Experimental values of N_b for α-helical transmembrane proteins are taken from Marsh and Horváth (1998), where references to the original work can be found.

Molecular modeling

Swiss-Pdbviewer (Guex and Peitsch 1997) was used for preparing and viewing protein structures. The position and orientation of the transmembrane domain were determined from the region of the protein that is poor in tryptophan, tyrosine, and charged residues. These identifications essentially agree with those given in the PDB_TM (Tusnády et al. 2004) and OPM (Lomize et al. 2006) databases. The starting configuration for the myr_2PtdCho lipid was molecule B from Pearson and Pascher (1979). A continuous bilayer ring of lipids was constructed around the protein. The interactive molecular mechanics package Sculpt 2.1 (Interactive Simulations Inc.) with default force field was used for building and optimizing lipid shells. Adjustment of the phospholipid chain configuration and constrained molecular mechanics optimization of the protein–lipid assemblies in vacuo were performed within Sculpt. Inward-directed forces were applied to all atoms of each lipid in order to pack the lipids on the protein surface. These forces were provided by the spring feature in Sculpt. One end of each spring was anchored in the protein, and the strength of the inward force was proportional to the length of the spring. The energy of the protein–lipid system (excluding the spring energy) was monitored as the springs pulled the lipids onto the protein surface. An energy minimum was thus achieved that would correspond approximately to equilibrium protein–lipid packing in the absence of the springs. Lipids were added to, or removed from, the final assembly, as required for close packing at the protein surface, with subsequent reoptimization. The PyMOL molecular graphics system (DeLano 2002) was used for presentation of structures. All modeling work was performed on a Silicon Graphics Origin 2000 server and O2 workstations.

Acknowledgments

Partial support from the Hungarian Scientific Research Fund (grant no. T-043425 to T.P.) is gratefully acknowledged. T.P. and D.M. are members of the COST D22 Action of the European Union.

References

Arora, A., Williamson, I.M., Lee, A.G., and Marsh, D. 2003. Lipid–protein interactions with cardiac phospholamban studied by spin-label electron spin resonance. *Biochemistry* **42:** 5151–5158.

Bashtovyy, D., Marsh, D., Hemminga, M.A., and Páli, T. 2001. Molecular modelling studies on the spin-labelled major coat protein of the M13 bacteriophage in a phospholipid bilayer. *Protein Sci.* **10:** 979–987.

Berman, H.M., Westbrook, J., Feng, Z., Gilliland, G., Bhat, T.N., Weissig, H., Shindyalov, I.N., and Bourne, P.E. 2000. The Protein Data Bank. *Nucleic Acids Res.* **28:** 235–242.

Bloom, M. and Smith, I.C.P. 1985. Manifestations of lipid–protein interactions in deuterium NMR. In *Progress in protein–lipid interactions* (eds. A. Watts and J.J.H.H.M. de Pont), Vol. 1, pp. 61–88. Elsevier, Amsterdam.

Brophy, P.J., Horváth, L.I., and Marsh, D. 1984. Stoichiometry and specificity of lipid–protein interaction with myelin proteolipid protein studied by spin-label electron spin resonance. *Biochemistry* **23:** 860–865.

Brotherus, J.R., Griffith, O.H., Brotherus, M.O., Jost, P.C., Silvius, J.R., and Hokin, L.E. 1981. Lipid–protein multiple binding equilibria in membranes. *Biochemistry* **20:** 5261–5267.

Cornea, R.L., Jones, L.R., Autry, J.M., and Thomas, D.D. 1997. Mutation and phosphorylation change the oligomeric structure of phospholamban in lipid bilayers. *Biochemistry* **36:** 2960–2967.

DeLano, W.L. 2002. *The PyMOL molecular graphics system*. DeLano Scientific, San Carlos, CA. http://www.pymol.org.

de Planque, M.R.R., Greathouse, D.V., Koeppe II, R.E., Schäfer, H., Marsh, D., and Killian, J.A. 1998. Influence of lipid/peptide hydrophobic mismatch on the thickness of diacylphosphatidylcholine bilayers. A ^{2}H NMR and ESR study using designed transmembrane α-helical peptides and gramicidin A. *Biochemistry* **37:** 9333–9345.

de Planque, M.R.R., Kruijtzer, J.A.W., Liskamp, R.M.J., Marsh, D., Greathouse, D.V., Koeppe II, R.E., De Kruijff, B., and Killian, J.A. 1999. Different membrane anchoring positions of tryptophan and lysine in synthetic transmembrane α-helical peptides. *J. Biol. Chem.* **274:** 20839–20846.

Ellena, J.F., Blazing, M.A., and McNamee, M.G. 1983. Lipid–protein interactions in reconstituted membranes containing acetylcholine receptor. *Biochemistry* **22:** 5523–5535.

Fajer, P., Knowles, P.F., and Marsh, D. 1989. Rotational motion of yeast cytochrome oxidase in phosphatidylcholine complexes studied by saturation-transfer electron spin resonance. *Biochemistry* **28:** 5634–5643.

Ferguson, A.D., Hofmann, E., Coulton, J.W., Diederichs, K., and Welte, W. 1998. Siderophore-mediated iron transport: Crystal structure of FhuA with bound lipopolysaccharide. *Science* **282:** 2215–2220.

Fraser, R.D.B. and MacRae, T.P. 1973. *Conformation in fibrous proteins and related synthetic peptides.*. Academic Press, New York.

Gao, X., Wen, X., Yu, C.-A., Esser, L., Tsao, S., Quinn, B., Zhang, L., Yu, L., and Xia, D. 2002. The crystal structure of mitochondrial cytochrome *bc1* in complex with famoxadone: The role of aromatic–aromatic interaction in inhibition. *Biochemistry* **41:** 11692–11702.

Guex, N. and Peitsch, M.C. 1997. Swiss model and the Swiss-Pdb viewer: An environment for comparative protein modeling. *Electrophoresis* **18:** 2714–2723.

Hesketh, T.R., Smith, G.A., Houslay, M.D., McGill, K.A., Birdsall, N.J.M., Metcalfe, J.C., and Warren, G.B. 1976. Annular lipids determine ATPase activity of a calcium-transport protein complexed with dipalmitoyllecithin. *Biochemistry* **15:** 4145–4151.

Horváth, L.I., Drees, M., Beyer, K., Klingenberg, M., and Marsh, D. 1990. Lipid–protein interactions in ADP-ATP carrier/egg phosphatidylcholine recombinants studied by spin-label ESR spectroscopy. *Biochemistry* **29:** 10664–10669.

Huang, L., Cobessi, D., Tung, E.Y., and Berry, E.A. 2005. Binding of the respiratory chain inhibitor antimycin to the mitochondrial bc1 complex: A new crystal structure reveals an altered intramolecular hydrogen-bonding pattern. *J. Mol. Biol.* **351:** 573–597.

Jones, O.T., Eubanks, J.H., Earnest, J.P., and McNamee, M.G. 1988. A minimum number of lipids are required to support the functional properties of the nicotinic acetylcholine receptor. *Biochemistry* **27:** 3733–3742.

Kleinschmidt, J.H., Powell, G.L., and Marsh, D. 1998. Cytochrome *c*-induced increase of motionally restricted lipid in reconstituted cytochrome *c* oxidase membranes, revealed by spin-label ESR spectroscopy. *Biochemistry* **37:** 11579–11585.

Knowles, P.F., Watts, A., and Marsh, D. 1979. Spin label studies of lipid immobilization in dimyristoylphosphatidylcholine-substituted cytochrome oxidase. *Biochemistry* **18:** 4480–4487.

Lomize, M.A., Lomize, A.L., Pogozheva, I.D., and Mosberg, H.I. 2006. OPM: Orientations of Proteins in Membranes database. *Bioinformatics* **22:** 623–625.

Luecke, H., Schobert, B., Richter, H.-T., Cartailler, J.-P., and Lanyi, J.K. 1999. Structure of bacteriorhodopsin at 1.55 Å resolution. *J. Mol. Biol.* **291:** 899–911.

Mantripragada, S., Horváth, L.I., Arias, H.R., Schwarzmann, G., Sandhoff, K., Barrantes, F.J., and Marsh, D. 2003. Lipid–protein interactions and effect of local anesthetics in acetylcholine receptor-rich membranes from *Torpedo marmorata* electric organ. *Biochemistry* **42:** 9167–9175.

Marsh, D. 1982. Electron spin resonance: Spin label probes. In *Techniques in lipid and membrane biochemistry* (eds. J.C. Metcalfe and T.R. Hesketh), Vol.B4/II, pp. B426/1–B426/44. Elsevier, Amsterdam.

———. 1985. ESR spin label studies of lipid–protein interactions. In *Progress in protein–lipid interactions* (eds. A. Watts and J.J.H.H.M. de Pont), Vol.1, pp. 143–172. Elsevier, Amsterdam.

———. 1990. *Handbook of lipid bilayers*. CRC Press, Boca Raton, FL.
———. 1997. Stoichiometry of lipid–protein interaction and integral membrane protein structure. *Eur. Biophys. J.* **26:** 203–208.
Marsh, D. and Horváth, L.I. 1998. Structure, dynamics and composition of the lipid–protein interface. Perspectives from spin-labelling. *Biochim. Biophys. Acta* **1376:** 267–296.
Miyazawa, A., Fujiyoshi, Y., and Unwin, N. 2003. Structure and gating mechanism of the acetylcholine receptor pore. *Nature* **423:** 949–955.
Okada, T., Fujiyoshi, Y., Silow, M., Navarro, J., Landau, E.M., and Shichida, Y. 2002. Functional role of internal water molecules in rhodopsin revealed by X-ray crystallography. *Proc. Natl. Acad. Sci.* **99:** 5982–5987.
Oldfield, E. 1982. NMR of protein–lipid interactions in model and biological membrane systems. In *Membranes and transport* (ed. E.N. Martonosi) pp. 115–123. Plenum Press, New York.
Páli, T. and Marsh, D. 2001. Tilt, twist and coiling in β-barrel membrane proteins: Relation to infrared dichroism. *Biophys. J.* **80:** 2789–2797.
Páli, T., Finbow, M.E., Holzenburg, A., Findlay, J.B.C., and Marsh, D. 1995. Lipid–protein interactions and assembly of the 16-kDa channel polypeptide from *Nephrops norvegicus*. Studies with spin-label electron spin resonance spectroscopy and electron microscopy. *Biochemistry* **34:** 9211–9218.
Pates, R.D., Watts, A., Uhl, R., and Marsh, D. 1985. Lipid–protein interactions in frog rod outer segment disc membranes. Characterization by spin labels. *Biochim. Biophys. Acta* **814:** 389–397.
Pautsch, A. and Schulz, G.E. 2000. High-resolution structure of the OmpA membrane domain. *J. Mol. Biol.* **298:** 273–282.
Pearson, R.H. and Pascher, I. 1979. The molecular structure of lecithin dihydrate. *Nature* **281:** 499–501.
Pebay-Peyroula, E., Dahout-Gonzalez, C., Kahn, R., Trézéguet, V., Lauquin, G.J.M., and Brandolin, G. 2003. Structure of mitochondrial ADP/ATP carrier in complex with carboxyatractyloside. *Nature* **426:** 39–44.
Peelen, S.J.C.J., Sanders, J.C., Hemminga, M.A., and Marsh, D. 1992. Stoichiometry, selectivity, and exchange dynamics of lipid–protein interaction with bacteriophage M13 coat protein studied by spin label electron spin resonance. Effects of protein secondary structure. *Biochemistry* **31:** 2670–2677.
Pérez-Gil, J., Casals, C., and Marsh, D. 1995. Interactions of hydrophobic lung surfactant proteins SP-B and SP-C with dipalmitoylphosphatidylcholine and dipalmitoylphosphatidylglycerol bilayers studied by electron spin resonance spectroscopy. *Biochemistry* **34:** 3964–3971.
Powell, G.L., Knowles, P.F., and Marsh, D. 1985. Association of spin-labelled cardiolipin with dimyristoylphosphatidylcholine-substituted bovine heart cytochrome *c* oxidase. A generalized specificity increase rather than highly specific binding sites. *Biochim. Biophys. Acta* **816:** 191–194.
Ramakrishnan, M., Pocanschi, C.L., Kleinschmidt, J.H., and Marsh, D. 2004. Association of spin-labelled lipids with β-barrel proteins from the outer membrane of *Escherichia coli*. *Biochemistry* **43:** 11630–11636.
Ryba, N.J.P., Horváth, L.I., Watts, A., and Marsh, D. 1987. Molecular exchange at the lipid–rhodopsin interface: Spin-label electron spin resonance studies of rhodopsin–dimyristoyl phosphatidylcholine recombinants. *Biochemistry* **26:** 3234–3240.
Sankaram, M.B., Brophy, P.J., and Marsh, D. 1991. Lipid–protein and protein–protein interactions in double recombinants of myelin proteolipid apoprotein and myelin basic protein with dimyristoylphosphatidylglycerol. *Biochemistry* **30:** 5866–5873.
Schulz, G.E. 2002. The structure of bacterial outer membrane proteins. *Biochim. Biophys. Acta* **1565:** 308–317.
Silvius, J.R., McMillen, D.A., Saley, N.D., Jost, P.C., and Griffith, O.H. 1984. Competition between cholesterol and phosphatidylcholine for the hydrophobic surface of sarcoplasmic reticulum Ca^{2+}-ATPase. *Biochemistry* **23:** 538–547.
Surles, M.C., Richardson, J.S., Richardson, D.C., and Brooks Jr., F.P. 1994. Sculpting protein interactively: Continual energy minimization embedded in a graphical modeling system. *Protein Sci.* **3:** 198–210.
Toyoshima, C., Nakasako, M., Nomura, N., and Ogawa, H. 2000. Crystal structure of the calcium pump of sarcoplasmic reticulum at 2.6 Å resolution. *Nature* **405:** 647–655.
Tsukihara, T., Shimokata, K., Katayama, Y., Shimada, H., Muramoto, K., Aoyama, H., Mochizuki, M., Shinzawa-Itoh, K., Yamashita, A., Yao, M., et al. 2003. The low-spin heme of cytochrome *c* oxidase as the driving element of the proton-pumping process. *Proc. Natl. Acad. Sci.* **100:** 15304–15309.
Tusnády, G.E., Dosztányi, Z., and Simon, I. 2004. Transmembrane proteins in the Protein Data Bank: Identification and classification. *Bioinformatics* **20:** 2964–2972.
Valiyaveetil, F.I., Zhou, Y.F., and MacKinnon, R. 2002. Lipids in the structure, folding, and function of the KcsA K^+channel. *Biochemistry* **41:** 10771–10777.
Watts, A., Marsh, D., and Knowles, P.F. 1978. Lipid-substituted cytochrome oxidase: No absolute requirement of cardiolipin for activity. *Biochem. Biophys. Res. Commun.* **81:** 397–402.
Watts, A., Volotovski, I.D., and Marsh, D. 1979. Rhodopsin–lipid associations in bovine rod outer segment membranes. Identification of immobilized lipid by spin labels. *Biochemistry* **18:** 5006–5013.
Zingsheim, H.P., Neugebauer, D.C., Frank, J., Hanicke, W., and Barrantes, F.J. 1982. Dimeric arrangement and structure of the membrane-bound acetylcholine receptor studied by electron microscopy. *EMBO J.* **1:** 541–547.